Published in final edited form as:
Bone. 2009 May ; 44(5): 924–929. doi:10.1016/j.bone.2008.12.030.

Density and architecture have greater effects on the toughness of trabecular bone than damage

Jacqueline G. Garrison[1,2], **Constance L. Slaboch**[1], and **Glen L. Niebur**[1,2,*]

[1] Tissue Mechanics Laboratory, Department of Aerospace and Mechanical Engineering,

[2] Bioengineering Graduate Program, University of Notre Dame, Notre Dame, IN 46556

Abstract

Bone damage has been cited as an important aspect of bone quality. As such, understanding the effects of damage on the toughness of trabecular bone should provide insight into trabecular bone behavior during energy-limiting cases, such as falls. The effects of damage on the toughness of 35 bovine trabecular bone specimens was studied. Damage was induced by compressing the on-axis specimens to either 1.5% or 2.5% strain, followed by compression to 7.5% strain. The overloads resulted in significant decreases in both modulus and elastic toughness, with significantly greater decreases for the high-damage group than the low-damage group. Following damage, the elastic toughness of the high-damage group was also lower than the undamaged elastic toughness of the control group. In contrast, there was no detectable effect of damage level on toughness measured to 7.5% strain. Toughness increased linearly with BMD (R^2 = 0.50) and by a power law relationship with volume fraction (BV/TV) (R^2=0.65). Microarchitectural parameters also predicted the toughness in the absence of BV/TV or BMD. Toughness decreased with increasing slenderness ratio (Tb.Sp/Tb.Th) and structure model index (SMI) (R^2=0.68, multiple regression), again independent of damage level, suggesting that failure is influenced by trabecular buckling. Taken together, the results show that normal variations in toughness due to density and architecture dominate the changes due to damage at the levels induced in this study. Moreover, measuring toughness is sensitive to the final strain, as differences found in the elastic and initial plastic regions were undetectable at higher strains. The self-limiting nature of microcracks in trabecular bone, or the trabecular architecture itself, may inhibit microcracks from propagating to macroscopic trabecular fractures, thereby limiting the effect of damage on toughness and making it difficult to detect in comparison to normal population variability.

Keywords

Trabecular bone; toughness; trabecular architecture; microdamage; bone quality

Introduction

Osteoporosis is a skeletal disease characterized by low bone mass and architectural deterioration that leads to decreased bone strength and increased fracture risk [1]. Bone mineral density (BMD) is the standard clinical measure to quantify fracture risk. However, BMD, as

*Corresponding author. Tel: +574 631 3327; fax: +574 631 2144. Email address: gniebur@nd.edu (G.L. Niebur).

measured by DEXA, identifies only half of incident osteoporotic fractures [2]. As such, several other factors, often referred to as bone quality [3], must affect fracture risk. Material properties, collagen and mineral chemistry, and microarchitecture have all been suggested [4]. Another commonly cited aspect of bone quality is the microdamage burden. Microdamage occurs in vivo in the trabecular bone of vertebral bodies [5,6] and femoral heads [7,8]. Degradation of the tissue mechanical properties by microdamage incurred during a fall could also play a role in the reported increase in fracture risk following non-fracturing falls [9] or in so-called spontaneous fractures [10].

Microdamage can be induced experimentally by overloading, and is associated with modulus reductions. The mechanical properties of bovine [11–13] and human [14,15] trabecular bone degrade when overloaded. For example, the elastic modulus of bovine trabecular bone decreased when strains $\geq 1.0\%$ were applied, and the strength decreased for strains exceeding 2.5%, independent of initial modulus [11]. In human trabecular bone, the relative strength reduction was greater for specimens with lower apparent densities [14]. On-axis compressive overloads caused transverse modulus reductions of 35% in vertebral trabecular bone [15], and shear modulus reductions of 2.47% in bovine tibial trabecular bone [16], indicating a dependence on loading orientation and mode. Modulus degradation is a direct measure of mechanical damage [17,18], which is related to microdamage accumulation in the bone tissue [12,13,19]. Microcrack density increases exponentially with increasing modulus reduction, and individual trabeculae begin to fracture at 2% applied strain [13].

While the strength and modulus of trabecular bone and their relation to density and damage have been studied, toughness has received less attention. Toughness represents a material's ability to absorb energy, and could be a relevant measure of bone's ability to withstand fracture during falls, which are energy-limited. The damage formation process acts as a toughening mechanism in human and bovine cortical bone [20]. However, pre-existing damage in canine ribs had a negative effect on the toughness in 3-point bending [21]. Indeed, a mechanically damaged material, all other things being equal, must have a lower toughness than the equivalent undamaged material. The goal of this study was to investigate the role of pre-existing microdamage in determining the toughness of trabecular bone along its principal mechanical axis. Specifically, the aims were to: 1) induce damage in trabecular bone samples; 2) compare the toughness of undamaged and damaged trabecular bone samples in uniaxial compression; and 3) quantify the relative effects of damage, density, and architecture on toughness.

1. Materials and methods

1.1. Specimen Preparation

Thirty-five on-axis cylindrical specimens were prepared from the proximal metaphyses of 22 bovine tibiae (approximately 2 years old). The axis of each specimen was aligned with the principal mechanical axis using micro-CT imaging combined with finite element analysis [22]. Briefly, a parallelepiped was cut from the bone and scanned at 30 μm resolution in a micro-CT scanner (μCT-80, Scanco Medical AG, Bassersdorf, Switzerland). The images were converted to micro-finite element models, which were used to find the principal mechanical axes [23]. A custom jig was used to align the sample, and a diamond coring drill (Starlite Industries, Bryn Mawr, PA) was used to cut a cylindrical sample aligned with the calculated principal mechanical axis. On average, the cylindrical axes of the specimen were only $7.32 \pm 3.24°$ (mean ± SD) from the principal fabric orientations with a median of 7.56°. The mean diameter and gage length of the specimens were 8.06 ± 0.17 mm and 22.12 ± 3.21 mm, respectively.

Prior to testing, the trabecular architecture of the specimens was quantified. The specimens were scanned by micro-CT at 20 μm isotropic resolution while saturated in buffered saline.

The scanning time was approximately one hour. Architectural parameters were computed using a model free method (μCT Evaluation program V4.3, Scanco Medical AG, Bassersdorf, Switzerland) (Table 1). The tissue bone mineral density (BMD_{Tissue}), which excludes the marrow space, and the apparent level BMD were measured using the scanner's calibration [24].

The samples were tested using techniques to minimize end artifacts. They were fixed in brass endcaps using cyanoacrylate glue (Prism 401, Loctite, Newington, CT) [25]. The effective gage length was taken as the exposed length plus one-half of the embedded length of the specimen for all strain measurements [25]. The marrow was removed to facilitate gluing, but this should not affect the mechanical properties at the strain rates studied [26]. The prepared specimens were wrapped in gauze saturated with saline, and stored at −20°C in airtight containers until mechanical testing.

1.2. Mechanical Testing

Specimens were assigned to one of three groups for testing based on apparent density ($p=0.75$, ANOVA). Group I was a control group (n=12), while groups II (n=12) and III (n=11) were low-and high-damage groups, respectively. Three nondestructive compressive loads to 0.4% strain were applied to measure the initial elastic modulus (E_i). Samples in groups II and III were then overloaded to either 1.5% (low) or 2.5% (high) strain, then returned to zero load. These strains produce significantly different levels of mechanical damage in this type of bone, as measured by modulus reduction [13]. Three additional non-destructive load cycles were applied to measure the damaged modulus (E_d) in groups II and III. To avoid unintended damage, group I was not subjected to these modulus measurement loads or a sham overload. Finally, all specimens were destructively loaded to 7.5% strain (Fig. 1).

All tests were performed at room temperature using an Instron model 8821s biaxial servo-hydraulic load frame (Instron Corp., Canton, MA) under strain control at a strain rate of 0.5% s^{-1}. Data were collected at 100 Hz. Specimens were kept hydrated at all times by wrapping in gauze saturated in buffered saline around the exposed length of the specimen.

The data were processed to determine the relevant mechanical properties, after noise reduction with a low pass filter (GCVSPL) [27]. The moduli were calculated from the derivative of quadratic curve fits from 0.0% to 0.2% strain at zero load on the stress-strain curves [28] and averaged for three loading curves. This method has been shown to be more precise than a linear fit to a portion of the stress strain curve [28]. The relative reduction between the undamaged and damaged modulus was used as a macroscopic measure of damage [29]. The undamaged and damaged strengths were determined by the local maximum value of stress reached during overloading and failure, respectively. The yield point was determined by the 0.2% offset method.

The initial and damaged elastic toughness ($U_{e,i}$ and $U_{e,d}$, respectively) were calculated as the area under the stress-strain curve to the yield point. Toughness was also calculated to 7.5% strain (U_t) (Fig. 2). Toughness was calculated using the trapezoid rule, summing at constant intervals of 0.01% strain. Linear and power law regressions were used to determine the dependence of toughness on density and architectural parameters.

Statistical analysis was performed with JMP IN 5.1 (SAS Institute Inc., Cary, NC), with a significance level of 0.05. Comparisons between groups were made using ANOVA with Tukey's post-hoc test. The mechanical properties were compared by ANCOVA to account for dependence on the architecture, density or modulus.

Five specimens were lost during mechanical testing. One specimen fractured prematurely when the extensometer slipped, and four specimens were not properly embedded.

2. Results

On average, the initial modulus (E_i) for all specimens was 1682 ± 691 MPa (mean ± SD), independent of group ($p = 0.22$, ANCOVA with BV/TV as covariate) (Table 2). The low overload resulted in relative modulus reductions for 9 of 10 specimens and the high overload for 10 of 10 specimens. One specimen in the low-damage group had a small increase in modulus (< 2%) but was included in the analysis, because no error in the preparation or testing could be identified. On average, the modulus decreased 9.65 ± 7.66% in the low-damage group compared to 19.47 ± 11.17% in the high-damage group ($p = 0.03$, ANOVA, Fig. 3a), independent of BMD and architecture ($p > 0.07$, ANCOVA). The secant modulus, defined as the quotient of the stress at maximum strain and the maximum applied strain during the overload [13], decreased by 50.8 ± 11.8% and 70.4 ± 6.4%, on-average, in the low-and high-damage groups, respectively ($p = 0.0002$, ANOVA).

The overloads decreased the strength of the samples. During the initial overload, the ultimate strength was only reached for specimens in the high-damage group (Fig. 2). In this group, the strength decreased by 24.75 ± 13.98% ($p = 0.0009$, paired t-test), independent of BMD or architecture ($p > 0.60$, ANOVA). Although the specimens in the low-damage group did not reach their ultimate strength during the overload, seven of ten reached a higher maximum stress during the overload than during the final failure load, indicating that the ultimate strength before damage would have been higher. The average maximum stress was 6.25 ± 15.46% higher than the ultimate stress following damage. Only two of 30 specimens were completely fractured at 7.5% compressive strain.

On average, the damaged elastic toughness ($U_{e,d}$) was smaller compared to the initial elastic toughness ($U_{e,i}$) in both the low- and high-damage groups. After overloading, the elastic toughness decreased from 0.033 ± 0.012 to 0.024 ± 0.012 mJ/mm^3 and from 0.050 ± 0.023 mJ/mm^3 to 0.022 ± 0.011 mJ/mm^3 in the low- and high-damage group, respectively ($p < 0.01$, paired t-test, Table 2). The relative reduction in the elastic toughness of the high-damage group was greater than the low-damage group ($p = 0.01$, ANOVA, Fig. 3b).

The measured toughness to 7.5% strain (U_t) increased linearly with increasing BMD ($R^2 = 0.50$, $p < 0.001$) and nonlinearly with increasing volume fraction (BV/TV) ($R^2 = 0.65$, $p < 0.001$, power law regression, Fig. 4). U_t did not depend on the damage level ($p=0.58$, ANCOVA, with BMD as a covariate). Post-hoc power analysis showed that an additional 45 samples per group would be necessary to detect differences between groups.

U_t was correlated to a number of architectural measures. Toughness increased with BMD_{Tissue} ($R^2 = 0.13$, $p < 0.05$), trabecular thickness (Tb.Th) ($R^2 = 0.53$, $p < 0.001$) and degree of anisotropy (DA) ($R^2 = 0.25$, $p = 0.005$). U_t decreased with structure model index (SMI) ($R^2 = 0.61$, $p < 0.001$) and slenderness ratio, which was defined as the ratio of Tb.Sp/Tb.Th ($R^2=0.59$, $p < 0.001$, Table 3). This ratio is analogous to the slenderness ratio in the Euler buckling formulae, and was used to detect increased susceptibility to buckling.

To determine whether combinations of architectural parameters also played a role in toughness, multiple linear regression was used. Two parameters that could mechanistically explain trabecular collapse were considered: slenderness ratio and SMI. Trabecular number (Tb.N) was not considered because it is highly correlated to Tb.Sp ($p < 0.001$). Similarly, connectivity density (Conn.D.) was correlated to both Tb.Sp ($p = 0.0001$) and Tb.Th ($p = 0.01$), while DA was correlated to Tb.Th ($p = 0.0002$) and SMI ($p = 0.004$). Therefore, only SMI, Tb.Sp, and Tb.Th were included with the latter two combined as the slenderness ratio. The toughness

depended on both the slenderness ratio ($p = 0.03$) and SMI ($p = 0.01$) (R^2=0.68, Fig. 5). The multiple regression resulted in an R^2 value greater than that for the univariate regression with BV/TV as well as BMD.

3. Discussion

Understanding the effects of damage on the failure behavior of trabecular bone is important for elucidating its role in osteoporosis and age related fragility. Microdamage accumulation has been associated with a degradation of material properties, but its role in fractures is not fully understood. As such, we sought to establish the relative effects of BMD, architecture, and damage on the toughness of trabecular bone. Because of the destructive nature of the tests, we did not directly measure microdamage, but instead used modulus reduction as a surrogate. The toughness of samples was dependent on the bone mineral density and on architectural parameters. In contrast, damage did not measurably affect the toughness to failure for on-axis loading, regardless of the magnitude of modulus reduction. Although the damaging loads decreased the modulus, strength, and elastic toughness, the overall toughness was primarily determined by the total strain to failure. This indicates that the normal variations in toughness due to density and architecture of trabecular bone are greater than the changes due to damage at the levels induced in this study. The effects of damage on toughness may be limited because formation of new damage dominates the propagation of existing microdamage in trabecular bone [12,13].

There are several notable strengths of this study. First, it considered the effects of damage on toughness, rather than strength. Because toughness represents a material's ability to absorb energy, the data provide better insight into the relative roles of the effects of damage and architecture on fractures due to falls, which are energy-limited. Second, the two strain levels were selected to induce damage to two levels to quantify the effects of damage and were based on reported data of trabecular bone yield and ultimate strains [13]. These strain levels have been shown to produce damage levels consistent with in vivo damage in human bone [12], and the presence of damage was verified by the decreases in modulus and elastic toughness. Finally, well-validated testing methods were used to ensure precision of measurements [25,28].

There are also several limitations to our experimental protocol that should be considered when interpreting the data. First, the specimens were taken from a single anatomic site with limited architectural variability. Additionally, the bone was taken from young animals and may not represent the aging human skeleton. However, the use of this bone eliminated the confounding effects of pre-existing damage and heterogeneity of mineralization, which would be unavoidable in human bone. The toughness was measured at a strain to 7.5% rather than to overt fracture. Indeed, only two of the 30 specimens actually fractured at this strain level. Moreover, identifying the fracture point during testing or by analyzing the data was inconsistent. We also investigated the differences in toughness measured to the ultimate strain (data not shown) and found no difference between overload and failure curves in the high-damage group. The lack of direct histological measurements to quantify the microdamage is also a limitation. However, based on existing literature, the level of microdamage in both damage groups would be expected to be greater than in the control group, as young bovine bone has almost no in vivo microdamage [12,13,19] while microdamage increases with increasing modulus reduction [13]. Finally, this study focused on damage in excised trabecular bone specimens. However, it is also important to understand the role of microdamage on the failure behavior of the whole bone at any anatomical site. The surrounding trabecular network and the cortical shell will also play a role in whole bone fracture. This study provides data that could be incorporated into such whole bone studies.

Measuring toughness in trabecular bone is sensitive to the protocol used. Although the elastic toughness significantly decreased following overloading, the toughness measured to the ultimate strain did not. Decreases in the ultimate stress were accompanied by increases in ultimate strain, resulting in no overall change in toughness to the ultimate stress. This suggests that changes in trabecular bone toughness measurements occur primarily in the elastic and initial plastic ranges, prior to the ultimate strain. Given the relatively small effects of microdamage on toughness to the ultimate and higher strains, the role of microdamage in trabecular bone quality may primarily be in the elastic behavior and its affect on stress redistribution in the whole bone.

Architectural parameters can provide insight into the mechanisms of trabecular bone toughness, but the effects can be obscured by those of BV/TV, which is highly correlated to several relevant architectural parameters. We found that SMI and trabecular slenderness were the key architectural features to determine toughness. The sensitivity of the toughness to each parameter was quantified by substituting the mean values into the relationships and varying each parameter by one standard deviation. A one standard deviation increase in BV/TV and BMD resulted in a 31.0% and 27.4% increase in toughness, respectively. Toughness was similarly sensitive to changes in slenderness, with a one standard deviation decrease resulting in a 18.3% increase in toughness, while a decrease in SMI led to a 16.2% increase in toughness. In contrast, the decrease in elastic toughness due to damage averaged 34.2 ± 19.7% and 54.9 ± 12.7% for the low- and high-damage groups, respectively.

Together, SMI and slenderness ratio can be interpreted in the context of cellular solid modeling [30]. Decreasing trabecular slenderness results in plastic yielding of the trabeculae rather than buckling [30], and hence a greater energy absorption. Similarly, lower SMI indicates a transition to a network of plates, which are subject to buckling along a single axis whereas rods are less constrained. In large-deformation finite element analysis of human trabecular bone, such a transition from plates to rods was the primary factor mediating the failure mechanisms of trabecular bone [31].

Mechanical damage, rather than microdamage, was used to differentiate between groups in this study. However, propagation of microcracks into trabecular fractures would be one expected mechanism of toughness degradation. As such, variability in microdamage levels within groups may have affected the outcome. Microdamage increases with increasing SMI, decreasing BV/TV, and decreasing Tb.Th in both mechanically damaged bovine trabecular bone [12] and in human vertebral trabecular bone [32]. These same variables affected the toughness in this study. However, even after correcting for these parameters, the effects of damage level were not detectable between groups. As such, accounting for the mechanical effects of microdamage using population-based studies may prove difficult, and highly controlled experimental designs are needed to reduce these effects.

The modulus reductions found in this study were lower than previous reports. Modulus reductions in bovine tibial trabecular bone compressed to 1.5% and 2.5% strain were 38.5% and 64.7%, respectively [11], compared to 9.6% and 24.3% here and in previous studies from our lab [12,16]. These differences are in part due to the method used to determine the modulus in this study [28] compared to earlier work [11,33]. Moduli measured from the initial slope of the stress strain curve are consistently higher than those measured using linear fits, and reflect the nonlinear elastic behavior of trabecular bone [28]. When the secant modulus at the end of overloading was used, as in previous studies [11,13], the modulus reductions were comparable.

The results complement a recent study where overloads did not significantly affect the strength or toughness of human vertebral trabecular bone in orthogonal loading directions [15]. Similarly, we found that the ultimate strengths following damage were not significantly

different between damage groups. Likewise, the damaged toughness measured to the ultimate strength was not significantly different between groups. However, in contrast to our results, these authors reported that on-axis toughness was correlated with Tb.N but not SMI, Tb.Th, or DA [15]. This may be attributed to the larger range of architectural parameters in our specimens. For example, the variation in SMI in these samples was over two times larger than in the samples studied by Badiei [15], which allows for stronger correlations. In addition, differences in tissue level behavior between aged human and young bovine trabecular bone may play a role.

In an in vivo study, treatment with raloxifene for 12 months increased the microdamage burden in dogs, indicated by a significantly higher mean crack length versus the control group. However, the toughness was unchanged or higher compared to controls in canine vertebral and femoral trabecular bone, respectively [34,35]. These results are consistent with the present findings that density and architecture are the primary contributors to trabecular bone toughness.

Taken together, the data provide insight into the mechanisms of fracture risk reduction by anti-resorptive treatments. Although these agents are known to increase the microdamage burden [36–39], they also increase bone mineral density [37,40–42] and prevent degradation of architecture [36,43]. For example, microdamage levels of 2.9 and 3.7 times that of controls were found in dogs treated with clinically relevant doses of risedronate and alendronate, respectively, which are similar to the effects reported in humans [44]. After normalizing for volume fraction, there was no significant difference in toughness between the treatment and vehicle groups, although the alendronate group tended toward significant differences in toughness [35]. In a more recent study, the energy to failure as a function of BMD was lower in alendronate treated dogs than in control or risedronate treated dogs [45]. As such, toughness may begin to decline at higher microdamage burdens. Moreover, the affects may be different in osteoporotic bone due to degradation of architecture and density. As such, additional controlled studies are warranted.

Acknowledgments

The publication was made possible through the support of the National Institutes of Health AR52008 and US ARMY Medical Research and Materiel Command PR054672.

References

1. Osteoporosis prevention, diagnosis, and therapy. J Am Med Assoc 2001;285:785–795.
2. Shuit S, van der Klift M, Weel A, de Laet C, Burger H, Seeman E. Fracture incidence and association with bone mineral density in elderly men and women: the Rotterdam Study. Bone 2004;34:195–202. [PubMed: 14751578]
3. Bouxsein ML. Bone quality: where do we go from here? Osteoporos Int 2003;14:118–127.
4. Burr DB, Forwood MR, Fyhrie DP, Martin RB, Shaffler MB, Turner CH. Bone microdamage and skeletal fragility in osteoporotic and stress fractures. J Bone Miner Res 1997;12:6–15. [PubMed: 9240720]
5. Wenzel TE, Shaffler MB, Fyhrie DP. In vivo trabecular microcracks in human vertebral bone. Bone 1996;19:89–95. [PubMed: 8853850]
6. Vashishth D, Koontz J, Qui SJ, Lundin-Cannon D, Yeni YN, Schaffler MB, Fyhrie DP. In vivo diffuse damage in human vertebral trabecular bone. Bone 2000;26:147–152. [PubMed: 10678409]
7. Villanueva ARJ, Longo AI, Weiner G. Staining and histomorphometry of microcracks in the human femoral head. Biotech Histochem 1994;69:81–88. [PubMed: 7515700]
8. Fazzalari NL, Forwood MR, Smith K, Manthey BA, Herreen P. Assessment of cancellous bone quality in severe osteoarthrosis: bone mineral density, mechanics, and microdamage. Bone 1998;22:381–388. [PubMed: 9556139]

9. Cummings R, Klineberg R. Fall frequency and characteristics and the risk of hip fractures. J Am Geriatr Soc 1994;42:774–778. [PubMed: 8014355]
10. Lauritzen JB. Hip fractures: Incidence, risk factors, energy absorption and prevention. Bone 1996;18:65S–75S. [PubMed: 8717550]
11. Keaveny TM, Wachtel EF, Guo XE, Hayes WC. Mechanical behavior of damaged trabecular bone. J Biomech 1994;27:1309–1318. [PubMed: 7798281]
12. Wang X, Niebur GL. Microdamage propagation in trabecular bone due to changes in loading mode. J Biomech 2006;39:791–790. [PubMed: 16488218]
13. Arthur-Moore TL, Gibson LJ. Microdamage accumulation in bovine trabecular bone in uniaxial compression. J Biomech Eng 2002;124:63–71. [PubMed: 11873773]
14. Keaveny TM, Wachtell EF, Kopperdahl DL. Mechanical behavior of human trabecular bone after overloading. J Orthop Res 1999;17:346–353. [PubMed: 10376722]
15. Badiei A, Bottema MJ, Fazzalari NL. Influence of orthogonal overload on human vertebral trabecular bone mechanical properties. J Bone Miner Res 2007;22:1690–1699. [PubMed: 17620053]
16. Wang X, Guyette J, Liu X, Roeder RK, Niebur GL. Axial-shear interaction effects on microdamage in bovine tibial trabecular bone. Eur J Morphol 2005;42:61–70. [PubMed: 16123025]
17. Davy, D.; Jepsen, K. Bone damage mechanics. In: Cowin, S., editor. The Bone Mechanics Handbook. CRC; New York: 2001. p. 18.1-18.25.
18. Jepsen, K.; Davy, D.; Akkus, O. Observations od damage in bone. In: Cowin, S., editor. The Bone Mechanics Handbook. CRC; New York: 2001. p. 17.1-17.8.
19. Wachtel EF, Keaveny TM. Dependence of trabecular damage on mechanical strain. J Orthop Res 1997;15:781–787. [PubMed: 9420610]
20. Vashishth D, Behiri JC, Bonfield W. Crack growth resistance in cortical bone: Concept of microcrack toughening. J Biomech 1997;30:763–769. [PubMed: 9239560]
21. Mashiba T, Hirano T, Turner CH, Forwood MR, Johnston CC, Burr DB. Suppressed bone turnover by bisphosphonates increases microdamage accumulation and reduces some biomechanical properties in dog rib. J Bone Miner Res 2000;15:613–620. [PubMed: 10780852]
22. Wang X, Liu X, Niebur GL. Preparation of on-axis cylindrical trabecular bone specimens using micro-CT imaging. J Biomech Eng 2004;126:122–125. [PubMed: 15171139]
23. van Rietbergen B, Odgaard A, Kabel J, Huiskes R. Direct mechanics assessment of elastic symmetries and properties of trabecular bone architecture. J Biomech 1996;29:1653–1657. [PubMed: 8945668]
24. Kazakia GJ, Burghardt AJ, Cheung S, Majumdar S. Assessment of bone tissue mineralization by conventional x-ray microcomputed tomography: comparison with synchrotron radiation microcomputed tomography and ash measurements. Med Phys. 2008accepted for publication
25. Keaveny TM, Pinilla TP, Crawford RP, Kopperdahl DL, Lou A. Systematic and random errors in compression testing of trabecular bone. J Orthop Res 1997;15:101–110. [PubMed: 9066533]
26. Carter DR, Hayes WC. The compressive behavior of bone as a two-phase porous material. J Bone Joint Surg 1977;59A:954–962. [PubMed: 561786]
27. Woltring HJ. A Fortran package for generalized, cross-validatory spline smoothing and differentiation. Adv Engng Software 1986;8:104–117.
28. Morgan EF, Yeh OC, Chang WC, Keaveny TM. Nonlinear behavior of trabecular bone at small strains. J Biomech Eng 1999;123:1–9. [PubMed: 11277293]
29. Krajcinovic, D.; Lemaitre, J. Continuum Damage Mechanics: Theory and Applications. New York: Springer-Verlag; 1987. p. 294
30. Gibson LJ. Biomechanics of cellular solids. J Biomech 2005;38:377–399. [PubMed: 15652536]
31. Bevill G, Eswaran SK, Gupta A, Papadopoulos P, Keaveny TM. Influence of bone volume fraction and architecture on computed large-deformation failure mechanisms in human trabecular bone. Bone 2006;39:1218–1225. [PubMed: 16904959]
32. Arlot ME, Burt-Pichat B, Roux J-P, Vashishth D, Bouxsein ML, Delmas PD. Microarchitecture influences microdamage accumulation in human vertebral trabecular bone. J Bone Miner Res 2008;23:1613–1618. [PubMed: 18518771]
33. Keaveny T. Mechanistic approaches to analysis of trabecular bone. Forma 1997;12:267–275.

34. Allen MR, Hogan HA, Hobbs WA, Koivuniemi AS, Koivuniemi MC, Burr DB. Raloxifene enhances material-level mechanical properties of femoral cortical and trabecular bone. Endocrinology 2007;148:3909–3913.
35. Allen MR, Iwata K, Sako M, Burr DB. Raloxifene enhances vertebral mechanical properties independent of bone density. Bone 2006;39:1130–1135. [PubMed: 16814622]
36. Komatsubara S, Mori S, Mashiba T, Ito M. Long-term treatment of incadronate disodium accumulates microdamage but improves the trabecular bone architecture in dog vertebra. J Bone Miner Res 2003;18:512–520. [PubMed: 12619936]
37. Mashiba T, Turner CH, Hirano T, Forwood MR, Johnston CC, Burr DB. Effects of suppressed bone turnover by bisphosphonates on microdamage accumulation and biomechanical properties in clinically relevant skeletal sites in beagles. Bone 2001;28:524–531. [PubMed: 11344052]
38. Allen MR, Iwata K, Phipps R, Burr DB. Alterations in canine vertebral bone turnover, microdamage accumulation, and biomechanical properties following 1-year treatment with clinical treatment doses of risedronate or alendronate. Bone 2006;39:872–879. [PubMed: 16765660]
39. Stepan JJ, Burr DB, Pavo I, Sipos A, Michalska D, Li J, Fahrleitner-Pammer A, Petto H, Westmore M, Michalsky D, Sato M, Dobnig H. Low bone mineral density is associated with bone microdamage accumulation in postmenopausal women with osteoporosis. Bone 2007;41:378–385. [PubMed: 17597017]
40. Fogelman I, Ribot C, Smith R, Ethgen D, Sod E, Reginster J-Y. Risedronate reverses bone loss in postmenopausal women with low bone mass: Results from a multinational, double-blind, placebo-controlled trial. J Endocrinol Metab 2000;85:1895–1900.
41. Harris ST, Watts NB, Genant HK, McKeever CD. Effects of risedronate treatment on vertebral and nonvertebral fractures in women with postmenopausal osteoporosis. J Am Med Assoc 1999;282:1344–1352.
42. Bonnick S, Saag KG, Kiel DP, McClung M, Hochberg M, Burnett S-AM, Sebba A, Kagan R, Chen E, Thompson DE, Papp AED. Comparison of weekly treatment of postmenopausal osteoporosis with alendronate versus risedronate over two years. J Endocrinol Metab 2006;91:2631–2637.
43. Dufresne T, Chmielewski P, Manhart M, Johnson T, Borah B. Risedronate preserves bone architecture in early postmenopausal women in 1 year as measured by three-dimensional microcomputed tomography. Calcif Tissue Int 2003;73:423–432. [PubMed: 12964065]
44. Liberman UA, Weiss SR, Broll J, Minne HW, Quan H, Bell NH, Rodriguez-Portales J, Downs RW, Dequeker J, Favus M, Seeman E, Recker RR, Capizzi T, Santora AC, Lombardi A, Shah RV, Hirsch LJ, Karpf DB. Effect of oral alendronate on bone mineral density and the incidence of fractures in postmenopausal osteoporosis. N Engl J Med 1995;333:1437–1443. [PubMed: 7477143]
45. Allen MR, Burr DB. Changes in vertebral strength-density and energy-absorption density relationships following bisphosphonate treatment in beagle dogs. Osteoporos Int 2008;19:95–99. [PubMed: 17710353]

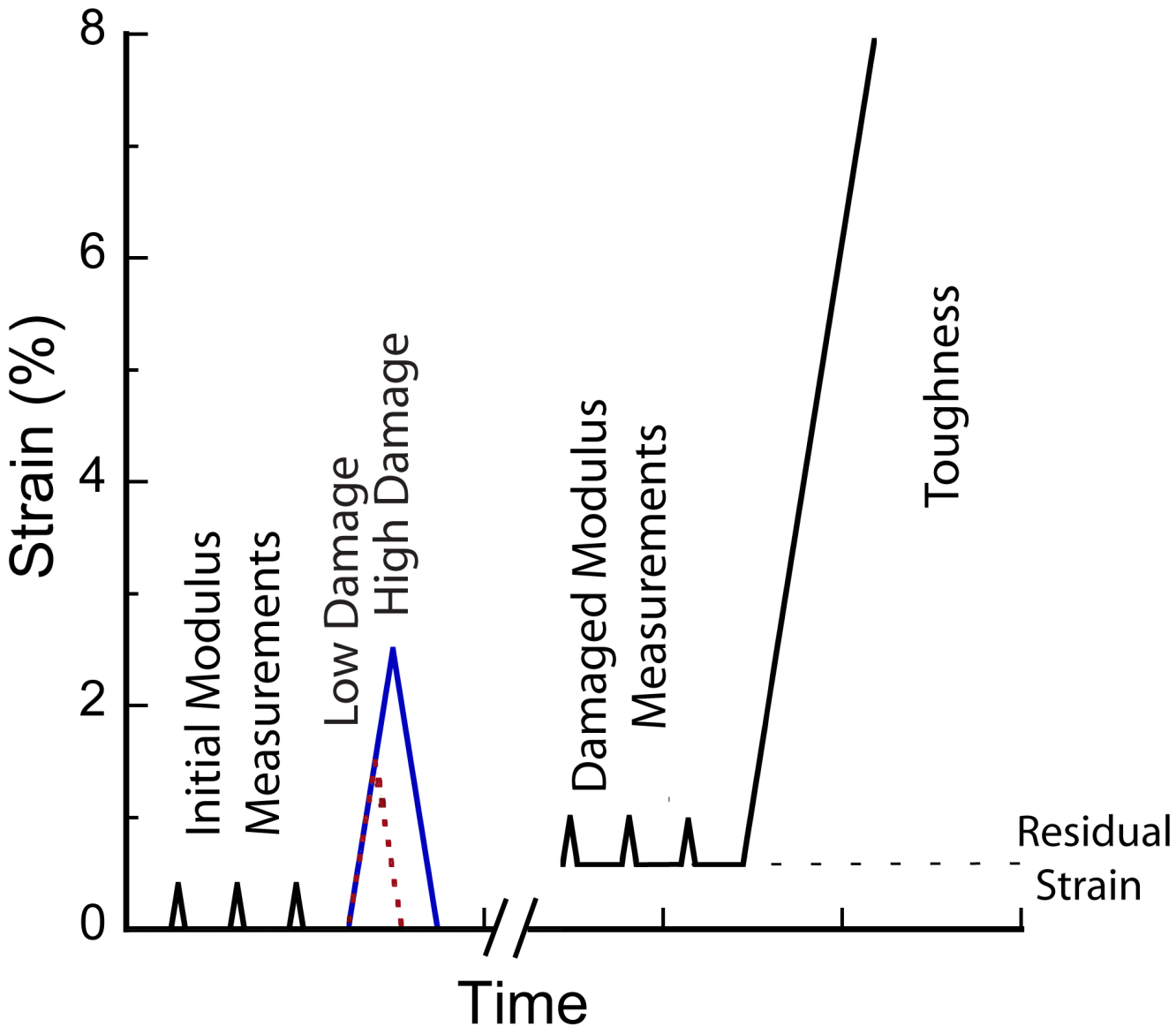

Figure 1.
Testing protocol for overloading specimens in uniaxial compression. Following the overload, the samples were unloaded to zero force resulting in a residual strain, which was the baseline strain for subsequent modulus and toughness measurements, indicated by the horizontal dashed line. To avoid unintentional damage, the control group was subjected to only the three modulus measurements and the final load to failure.

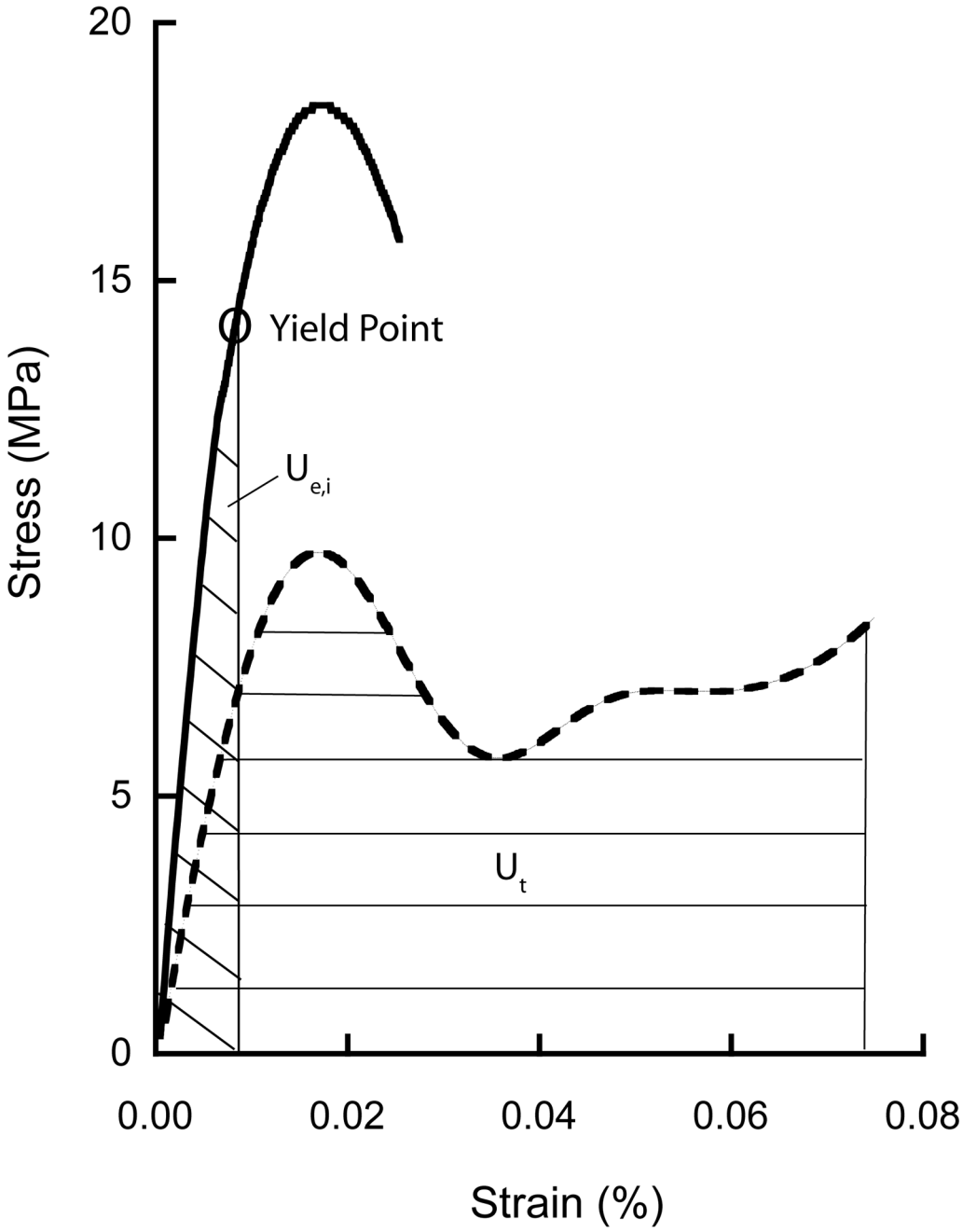

Figure 2.
Representative curve of stress-strain behavior for typical on-axis specimen subject to initial overload of 2.5% strain (solid line) and then to failure of 7.5% strain (dashed line). The initial elastic toughness ($U_{e,i}$) and toughness to 7.5% strain (U_t) are indicated by shading on the graph. $U_{e,i}$ was measured using the yield strain based on the 0.2% offset method.

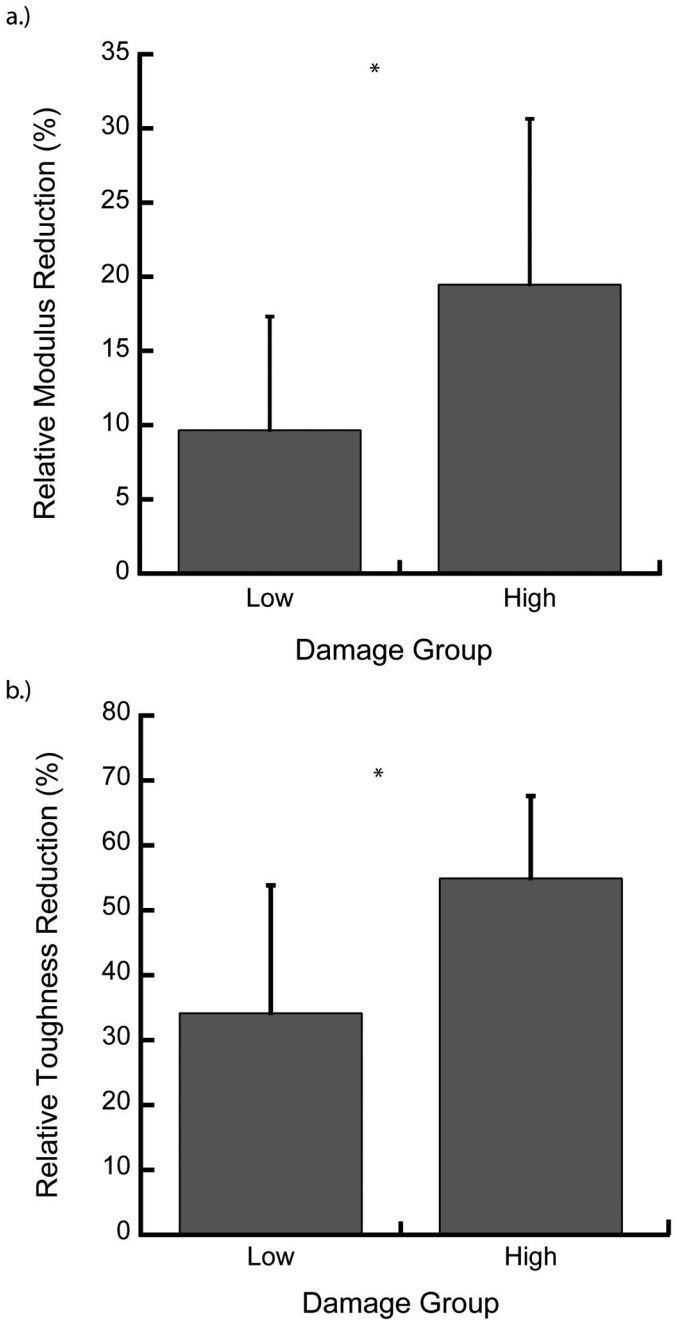

Figure 3.
The relative modulus (a) and elastic toughness (b) reductions were greater in the high- vs low-damage group (*$p < 0.04$). The modulus increased for one specimen in the low-damage group, but the mean modulus and elastic toughness decreased for both the low-and high-damage groups (paired t-test). Error bars are one S.D.

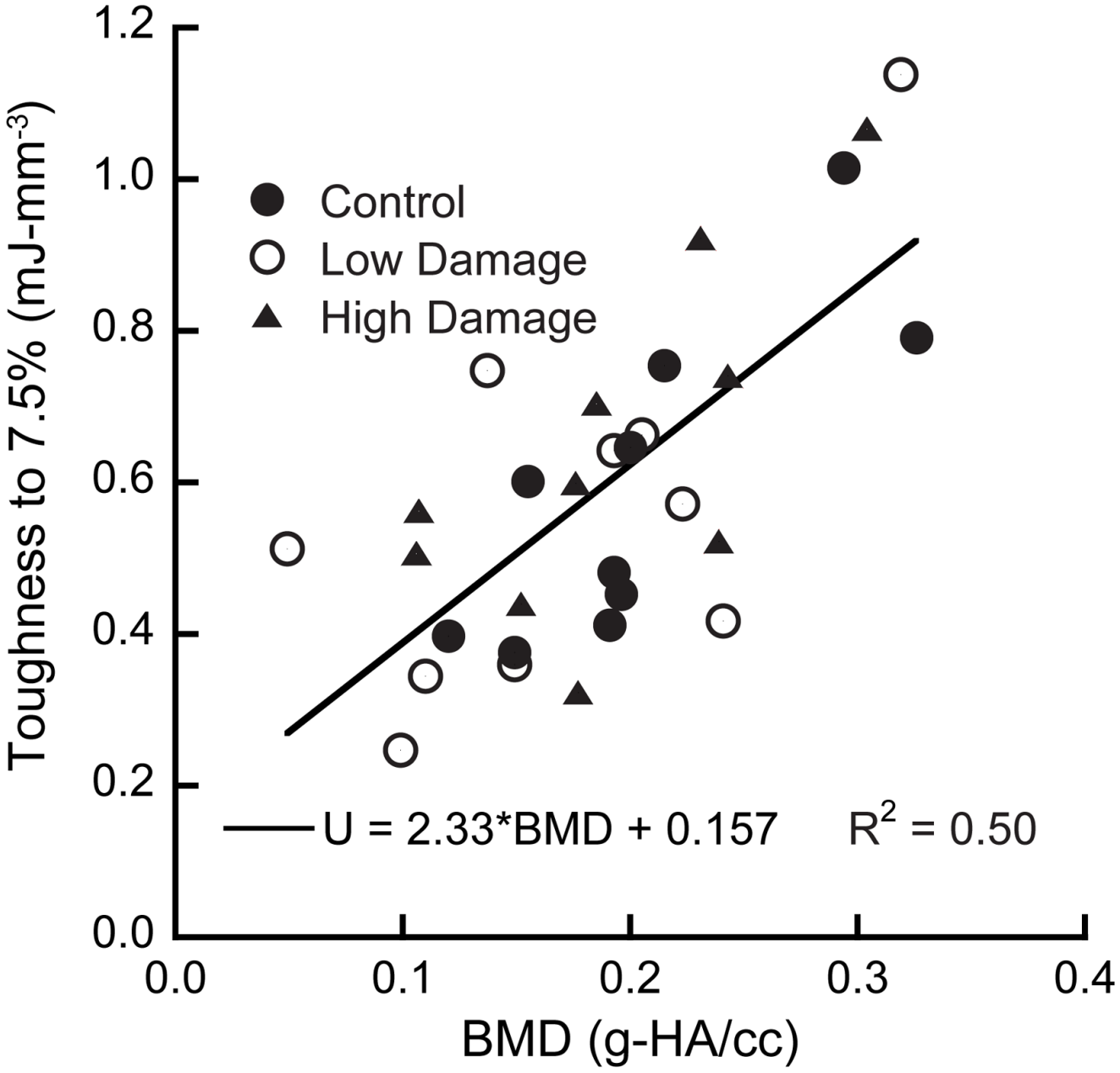

Figure 4.
Toughness to 7.5% compressive strain (U_t) increased with increasing BMD ($p < 0.001$) independent of damage level ($p = 0.58$).

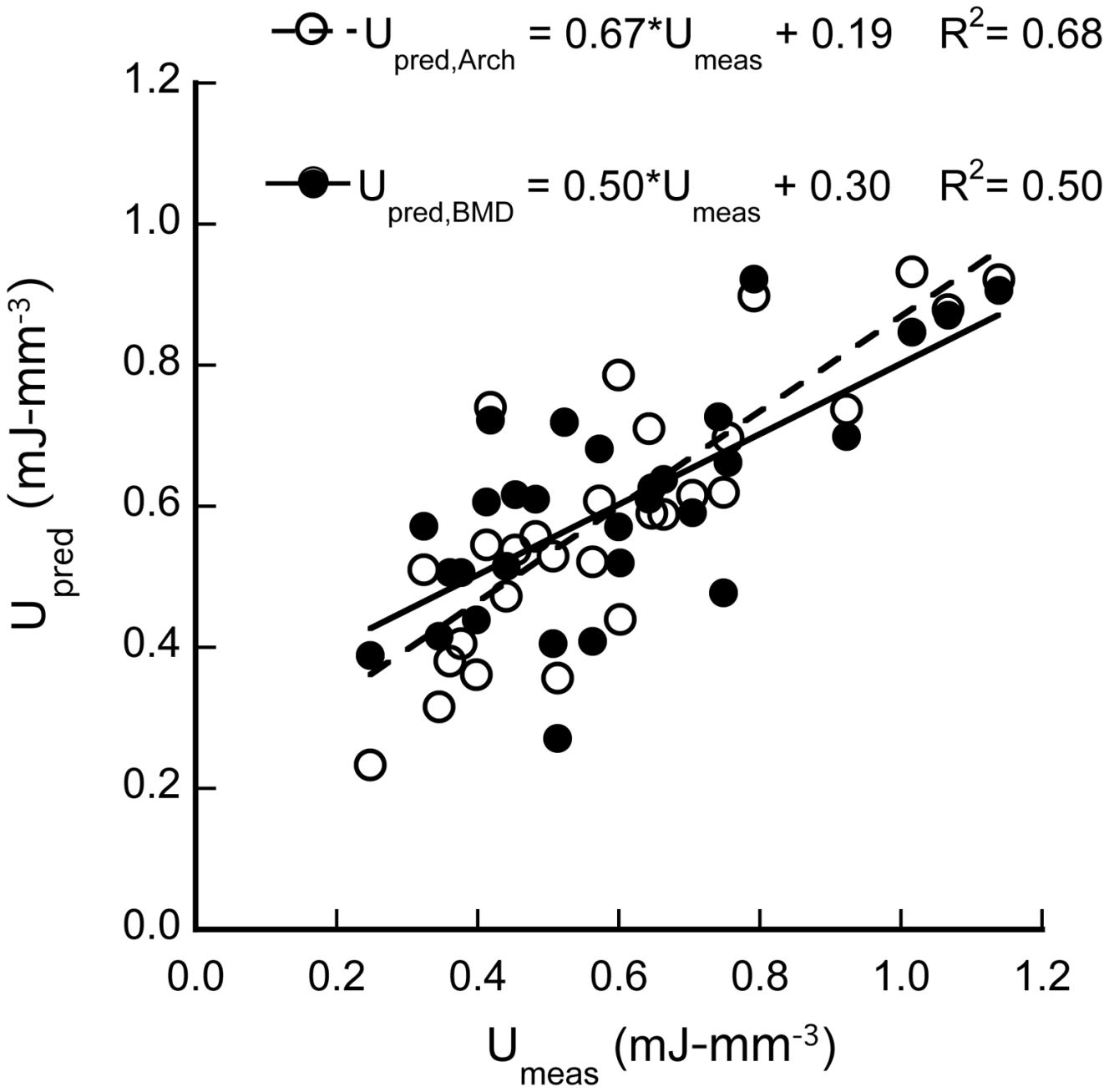

Figure 5.
Multiple regression with microarchitectural parameters resulted in a higher R^2 value than BMD alone when predicting the toughness of trabecular bone. $U_{pred,Arch} = -0.22*SMI - 0.14*Tb.Sp/Tb.Th + 1.27$ and $U_{pred,BMD} = 2.33*BMD + 0.157$.

Table 1

Trabecular density and architecture of the specimens quantified using micro-CT (n=30).

Parameters[1]	**Mean**	**SD**	**Range**
BMD (g-HA/cc)	0.189	0.068	0.049 – 0.326
BMD_{Tissue} (g-HA/CC)	0.872	0.027	0.822 – 0.931
BV/TV	0.244	0.058	0.147 – 0.376
Tb.N (mm^{-1})	1.501	0.136	1.199 – 1.856
Tb.Th (mm)	0.186	0.037	0.139 – 0.278
Tb.Sp (mm)	0.589	0.059	0.452 – 0.767
Tb.Sp/Tb.Th	3.324	0.628	2.202 – 4.802
SMI	0.922	0.499	0.046 – 1.924
Conn.D, (mm^{-3})	7.045	2.587	3.052 – 14.497
DA	2.092	0.417	1.314 – 3.088

[1] BMD = bone mineral density, BV/TV= volume fraction, Tb.N = trabecular number, Tb.Sp = trabecular separation, Tb.Th/Tb.Sp = slenderness ration, SMI = structure model index, Conn. D. = connectivity density, and DA = degree of anisotropy. BMD and BMD_{Tissue} were measured on the total volume and bone tissue volume, respectively.

Table 2

Initial and damaged strength (S_i, S_d), modulus (E_i, E_d), elastic toughness ($U_{e,i}$, $U_{e,d}$) and toughness to 7.5% strain (U_t) of bovine trabecular bone subject to three prescribed damage levels (mean ± SD). P-values are based on ANCOVA between groups with initial modulus (E_i) as a covariate (unless otherwise noted). Levels not connected by the same letter are significantly different.

	Control	Low Damage	High Damage	Average	P
E_i (MPa)	1497 ± 619[1]	1710 ± 822	1537 ± 644	1682 ± 691	0.22[2]
E_d (MPa)	1497 ± 618	1586 ± 836	1453 ± 467	1512 ± 638	0.42[2]
S_i (MPa)	11.21 ± 3.46[1]	---	15.36 ± 6.42	13.28 ± 5.45	0.19
S_d (MPa)	11.21 ± 3.46	10.91 ± 4.99	11.61 ± 5.30	11.24 ± 4.50	0.20
$U_{e,i}$ (mJ-mm^{-3})	0.031± 0.008[1]	0.033 ± 0.012	0.050 ± 0.023	0.038 ± 0.018	0.08
$U_{e,d}$ (mJ-mm^{-3})	0.031 ± 0.008^{A}	0.024 ± 0.012^{AB}	0.022 ± 0.011^{B}	0.025 ± 0.011	**0.02**
U_t (mJ-mm^{-3})	0.593 ± 0.21	0.565 ± 0.26	0.639 ± 0.22	0.599 ± 0.23	0.32

[1] The initial strength and modulus for the control group were also used as the damaged values to allow for correlations across groups. However, only one modulus, elastic toughness, and strength measurement were performed on the control group.

[2] BVTV was used as the covariate for ANCOVA of the modulus measurements.

Table 3

P-values, coefficients of determination, and slopes from linear regression (unless otherwise noted) relating architectural parameters to toughness.

Parameters	Linear Regression	Multiple linear regression
BMD (g-HA/cc)	**p < 0.0001**	
	R^2 = 0.49	---
	Slope = 2.33	
BMD_{Tissue} (g-HA/cc)	**p < 0.05**	
	R^2 = 0.13	---
	Slope = 2.97	
BV/TV	**p < 0.0001**	
	R^2 = 0.65*	---

Tb.N. (mm^{-1})	p = 0.88	
	---	---

Tb.Th. (mm)	**p < 0.001**	
	R^2= 0.53	---
	Slope = 4.61	
Tb.Sp. (mm)	p = 0.27	
	---	---

Conn.D. (mm^{-3})	p = 0.25	
	---	---

DA	**p = 0.005**	
	R^2= 0.25	---
	Slope = 0.27	
Tb.Sp/Tb.Th	**p < 0.001**	**p = 0.03**
	R^2= 0.59	
	Slope = −0.28	Slope = −0.14
SMI	**p < 0.001**	**p = 0.01**
	R^2= 0.61	
	Slope = −0.37	Slope = −0.22

Significant values are bold.

*indicates power law relationship: $U_t = 3.46*BV/TV^{1.27}$